

## Direct numerical simulation of bifurcating jets

Ionut Danaila<sup>a)</sup> and Bendiks Jan Boersma<sup>b)</sup>  
*Center for Turbulence Research, Stanford, California 94305*

(Received 19 January 1999; accepted 13 December 1999)

The mechanisms leading to bifurcating jets are investigated by means of direct numerical simulation. Two distinct types of jets were obtained by applying a bi-modal perturbation at the nozzle. When forcing simultaneously the counter-rotating helical modes (flapping mode) with the same amplitude and the same frequency, the jet splits into two branches, taking a distinct *Y*-shape. A different evolution of the jet ( $\Psi$ -shape) is observed when superposing the axisymmetric mode at the most amplified unstable frequency on the flapping mode with the same amplitude, but subharmonic frequency. In both cases a spectacular increase of the jet spreading is observed.

© 2000 American Institute of Physics. [S1070-6631(00)00404-9]

Bifurcating jets, which split into two distinct branches, are of particular interest for many practical applications, due to their increased spreading angle and mixing properties. Early experiments of Lee and Reynolds<sup>1</sup> and Parekh *et al.*<sup>2</sup> showed that a dual-mode, dual-frequency forcing is needed to produce a bifurcating jet. The required condition for bifurcation was an axial forcing frequency equal to twice the helical-type (orbital<sup>1</sup> or flapping<sup>2</sup>) forcing frequency. Bifurcation occurred only within a limited range of axial Strouhal numbers ( $St_0$ ), slightly depending on the Reynolds number ( $St_0=0.35-0.7$  for  $Re=2800-10\,000$  and  $St_0=0.3-0.65$  for  $Re=10\,000-100\,000$ ).

Similar (albeit more distorted) bifurcating jets were also reported in jet experiments using axial forcing and passive control devices. Stepped or sawtooth trailing edges attached at the nozzle exit<sup>3</sup> or inclined nozzles<sup>4</sup> generated complex helical structures which altered the downstream evolution of vortex rings. The bifurcating effect was found to be strongest when low forcing frequencies were used. Bifurcating supersonic jets were obtained by a combination of two diametrically opposed tabs placed at the nozzle exit.<sup>5</sup>

In this work we make use of direct numerical simulation (DNS) to assess the influence of the modal distribution of the forcing on the dynamics of the bifurcating jet. Two types of excitations leading to bifurcating jets are considered: *flapping* (F) excitation (containing the helical  $m=\pm 1$  modes with the same frequency and amplitude) and *bifurcating* (BF) excitation (superposition of the axisymmetric  $m=0$  mode on the flapping mode with the same amplitude, but subharmonic frequency). It should be noted that experiments of Parekh *et al.*<sup>2</sup> mainly used (BF)-type excitations to trigger bifurcating jets. The (F)-type excitation was not experimentally documented in this context.

The numerical solver simulates a free round jet issuing from a circular orifice of diameter  $D$  in a solid wall. The

incompressible Navier–Stokes equations are solved in a spherical coordinate system, with  $(r, \theta, \phi)$  denoting the radial, azimuthal and tangential directions. Details of the numerical scheme can be found in Boersma *et al.*<sup>6</sup> The three-dimensional computational domain has a streamwise extent of  $15D$  and a spanwise diameter of  $3D$  for the inflow section and  $10D$  for the outflow section. At the inflow section, the mean streamwise velocity profile is imposed as initial and boundary condition. We used the classical hyperbolic tangent ( $\tanh$ ) profile, which matches very well with profiles measured in experiments.<sup>2</sup> At the lateral boundary, traction-free boundary conditions allow fluid exchange across the boundary. The so-called convective boundary condition<sup>7</sup> was used at the downstream boundary.

The Reynolds number, based on diameter, is fixed to  $Re=1500$  and the jet parameter to  $D/\Theta_0=60$  ( $\Theta_0$  is the initial momentum thickness). For these physical parameters and for the considered computational domain, a mesh of  $(192 \times 128 \times 96)$  grid-points in the  $(r, \theta, \phi)$  directions is sufficient to resolve the smallest scales of the motion.<sup>6</sup>

The simulated jet is forced by superposing oscillating components on the mean nozzle exit velocity. Only streamwise velocity disturbances are used. For convenience, the cylindrical coordinates  $(r_c, \theta_c, z)$  with  $r_c$  the radial,  $\theta_c$  the azimuthal, and  $z$  the streamwise directions, are used to describe the inflow velocity profile:

$$\frac{V_z}{V_{z0}} = 1 + \sum_m A_m \sin(2\pi f_m t - m\theta_c + \Phi_m) \left(\frac{2r_c}{D}\right)^{|m|},$$

where  $V_{z0}$  is the mean  $\tanh$  inflow profile and  $A_m, f_m, \Phi_m$  are, respectively, the amplitude, frequency and relative phase of the excitation. The guidelines for the selection of excitation parameters in order to obtain bifurcating jets were found in Parekh *et al.*<sup>2</sup> (see Table I).

The response of the jet flow to the excitations described above is analyzed both instantaneously and statistically. As in experiments, flow visualization is emphasized. For this purpose, a passive scalar conservation equation with Fickian diffusion assumption is solved with the same numerical scheme.

<sup>a)</sup>Also at IRPHE, 12 Av. Général Leclerc, 13003 Marseille, France.

<sup>b)</sup>Corresponding author. Present address: Delft University of Technology, Rotterdamseweg 145, 2628 AL Delft, The Netherlands. Electronic mail: b.j.boersma@wbmt.tudelft.nl

TABLE I. Run cases (the Strouhal number is defined as  $St_m = f_m D / V_{z0}$ ).

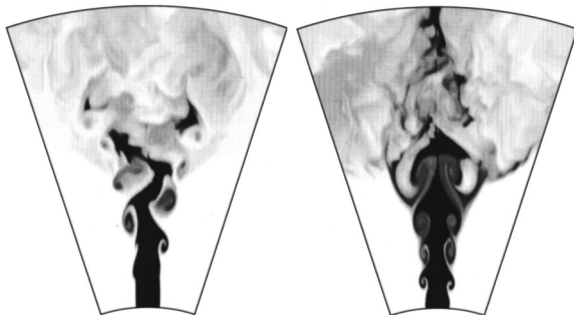
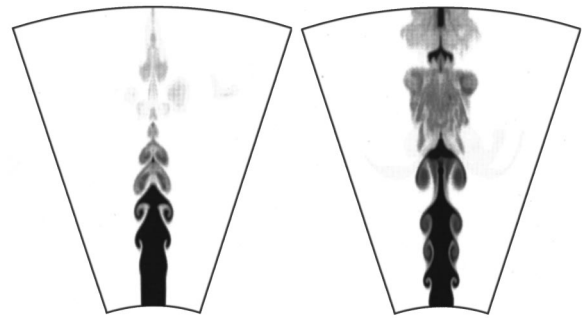
Case	Excitation
(F)	$A_{\pm 1} = 0.15$ ; $St_{\pm 1} = 0.55$ ; $\Phi_{+1} - \Phi_{-1} = 0$
(BF)	$A_0 = A_{\pm 1} = 0.15$ ; $St_0 = 2 \cdot St_{\pm 1} = 0.55$ ; $\Phi_0 - \Phi_{\pm 1} = \pi/4$

When flapping or bifurcating excitation are applied at the nozzle, a spectacular increase of the jet spreading angle is observed in the *bifurcating plane*. This plane of maximum spreading is fixed by the azimuthal position where the flapping perturbation locks ( $\theta_c = 0$  in our case). The plane perpendicular to the bifurcation plane is also called *bisecting plane*. Figure 1 depicts instantaneous pictures of the scalar evolution in the bifurcating plane for the jet with flapping (left) and bifurcating (right) perturbation. The same picture taken in the bisecting plane is presented in Fig. 2. Both jets exhibit different behavior in the two planes.

In the bifurcating plane, the flapping excitation determines the (F)-jet to split into two distinct branches (Fig. 1, left). Approximately at the same downstream location ( $z/D \approx 5$ ), the (BF)-jet spreads in a wide-angle turbulent structure (Fig. 1, right). In the bisecting plane, the scalar evolution is similar for both jets. The tracer is organized in large, symmetrically displayed structures, which seems to disappear downstream of  $z/D \approx 5$  (Fig. 1). Practically no spreading is observed in this plane.

This different evolution in two perpendicular planes is a characteristic of experimentally observed bifurcating jets. However, Parekh *et al.*<sup>2</sup> emphasized that a jet which spreads more rapidly in one plane than in the corresponding perpendicular plane is not necessarily a bifurcating jet, since elliptical jets exhibit the same characteristic. They proposed two criteria to define a bifurcating jet: the jet splits into two separate jets (i.e., the jet fluid disappears as one moves downstream in the bisecting plane) and/or the far-field streamwise velocity profiles consist of two separate peaks.

The surprising result displayed in our simulations was that only the (F)-jet fulfilled the two criteria, as shown in Figs. 3 and 4 presenting mean scalar fields and mean streamwise velocity profiles. The Y-shaped structure of the (F)-jet is clearly displayed in Fig. 3, while the tree-structure of the (BF)-jet can be generically described as  $\Psi$ -shaped.

FIG. 1. (F)-jet (left) and (BF)-jet (right). Snapshot of the passive scalar field in the bifurcating plane ( $\theta_c = 0$ ).FIG. 2. Same as in Fig. 1. Evolution in the bisecting plane ( $\theta_c = 90^\circ$ ).

This trend is different to that observed in experiments and need a detailed description. In experimental bifurcating jets, the combined axial and flapping forcing created a periodic array of vortex rings, which were alternatively shifted in the radial direction. The helical disturbances reached their maximum amplification at the end of the potential core. As a result, the rings tilted and propagated along two different trajectories.

In our simulated (F)-jet, a similar mechanism is involved. Ringlike vortical structures roll up in alternatively tilted planes every half-period of excitation. The cores of these structures progressively diminish towards the region of minimum perturbation amplitude. At this azimuthal location, the vortex ends do not merge in a toroidal loop; they bend downstream and merge with the next vortex, generating a large intertwined structure. This continuous structure breaks up at  $z/D \approx 5$ . As a result, vortex structures similar to distorted rings propagate along two distinct branches. This last phase of vortex evolution is similar to that observed in experiments. However, the initial stages of formation of the involved ring structures is different, since we never observed usual toroidal rings in our simulation.

A possible explanation for the successful generation of a bifurcating jet with a single-frequency flapping excitation is the use of a high amplitude forcing at the most linearly amplified frequency of the helical mode. Experiments of Corke and Kusek<sup>8</sup> showed that such combination led to resonant amplification of near-subharmonic helical modes, while using a forcing at half of the most linearly amplified frequency (as in experiments of Parekh *et al.*<sup>2</sup>) did not affect the natural instability modes.

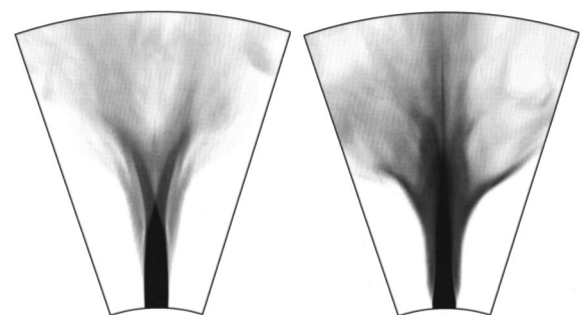


FIG. 3. (F)-jet (left) and (BF)-jet (right). Mean passive scalar field in the bifurcating plane.

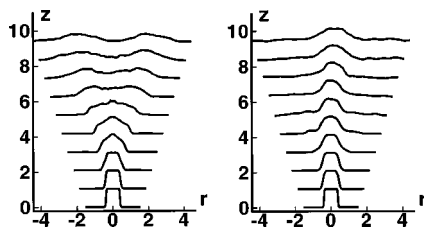


FIG. 4. (F)-jet (left) and (BF)-jet (right). Mean streamwise velocity profiles.

It is interesting to note that single-frequency streamwise velocity perturbation was applied in recent large-eddy simulations (LES) of Urbin *et al.*<sup>9</sup> to obtain high Reynolds number bifurcating jets. Their alternated-pairing excitation triggered tilted coherent vortex rings, which locally paired and finally spread in the excitation plane. The obtained jet spread more rapidly in the excitation plane than in the corresponding perpendicular plane, but the mean streamwise velocity field did not display the Y-shape required by the above-mentioned definition of a bifurcating jet.

A different mechanism is involved in the evolution of the (BF)-jet. The shear-layer rolls up into slightly tilted coherent vortex rings (Fig. 4, right). Farther downstream, the vortex ring undergoes strong azimuthal instabilities and finally breaks up into small and irregular vortex structures. As observed from Fig. 4, the tracer is ejected directly from the vortex sheet connecting the rings (braid region). This phenomenon can be explained by the excessive growth of streamwise filaments in the braid region.<sup>10</sup> The streamwise filaments are stretched by the high field strain and pulled outward from the jet by the moving vortex rings. The (BF)-jet displays a large spreading in the bifurcating plane, but it does not satisfy any of the criteria defining a bifurcating jet, since an important amount of fluid is observed downstream near the axis (Figs. 3 and 4).

This spreading mechanism, already documented in previous studies of heated and variable density jets,<sup>11</sup> is completely new in the context of bifurcating jets and it was not observed in experiments. As the Strouhal number of the numerical (BF) excitation is within the experimentally reported range leading to bifurcation, we can speculate that a strong coupling between the axial and flapping components of the excitation is responsible for inhibiting the bifurcation. The vortex rings generated by the strong axial perturbation are

only azimuthally distorted by the flapping excitation (containing only streamwise perturbations). No radial displacement or tilt of rings are induced. In experiments, the two components of the excitation are decoupled; the flapping perturbation also contains a transverse component which is more effective in radially displacing the rings and, therefore, triggering the bifurcation.

In conclusion, our numerical simulations have revealed two new interesting features, compared to experiments, of the forced jet when dual-mode excitation is used: (i) single-frequency flapping excitation can trigger Y-shaped bifurcating jets; (ii) usual bifurcating excitation (axial+flapping with different frequencies) can lead to large-spreading jets, which are not necessarily bifurcating jets. This is of particular interest for establishing control strategies since the two numerically obtained jets exhibit a large spreading rate and an enhanced mixing of the passive scalar.

## ACKNOWLEDGMENTS

This work was performed at the Center for Turbulence Research during the 1998 Summer Program. We acknowledge the helpful input of Professor W. C. Reynolds and Professor P. Moin in positioning this investigation. We also thank Professor D. Parekh for stimulating discussions.

- <sup>1</sup>M. Lee and W. C. Reynolds, "Bifurcating and blooming jets," Report No. TF-22, Department of Mechanical Engineering, Stanford University, 1985.
- <sup>2</sup>D. Parekh, A. Leonard, and W. C. Reynolds, "Bifurcating jets at high Reynolds numbers," Report No. TF-35, Department of Mechanical Engineering, Stanford University, 1988.
- <sup>3</sup>E. K. Longmire and L. H. G. Duong, "Bifurcating jets generated with stepped and saw-tooth nozzles," *Phys. Fluids* **8**, 978 (1995).
- <sup>4</sup>D. R. Webster and E. K. Longmire, "Vortex dynamics in jets from inclined nozzles," *Phys. Fluids* **9**, 655 (1997).
- <sup>5</sup>K. B. M. Q. Zaman, G. Raman, and M. Samimy, "Control of an axisymmetric jet using vortex generators," *Phys. Fluids* **6**, 778 (1994).
- <sup>6</sup>B. J. Boersma, G. Brethouwer, and F. T. M. Nieuwstadt, "A numerical investigation the effect of the inflow conditions on the self-similar region of a round jet," *Phys. Fluids* **10**, 899 (1998).
- <sup>7</sup>I. Orlanski, "A simple boundary condition for unbounded hyperbolic flows," *J. Comput. Phys.* **21**, 251 (1976).
- <sup>8</sup>T. C. Corke and S. M. Kusek, "Resonance in axisymmetric jets with controlled helical-mode input," *J. Fluid Mech.* **249**, 307 (1993).
- <sup>9</sup>G. Urbin, C. Brun, and O. Métais, "Large eddy simulation of three-dimensional spatially evolving round jets," in 11th Symposium on Turbulent Shear Flows, Grenoble, 1997, edited by Durst *et al.*
- <sup>10</sup>D. Liepmann and M. Gharib, "The role of streamwise vorticity in the near-field entrainment of round jets," *J. Fluid Mech.* **245**, 643 (1992).
- <sup>11</sup>See Monkewitz *et al.*, *Phys. Fluids A* **1**, 446 (1989); Sreenivasan *et al.*, *Exp. Fluids* **7**, 309 (1989).